

AD-A111 806

PANAMETRICS INC WALTHAM MASS F/G 20/8  
ANALYSIS OF THE RAM EFFECT OBSERVED WITH THE ELECTRON ESA ON TH—ETC(U)  
NOV 81 F A HANSER, B SELLERS F19628-79-C-0009

UNCLASSIFIED

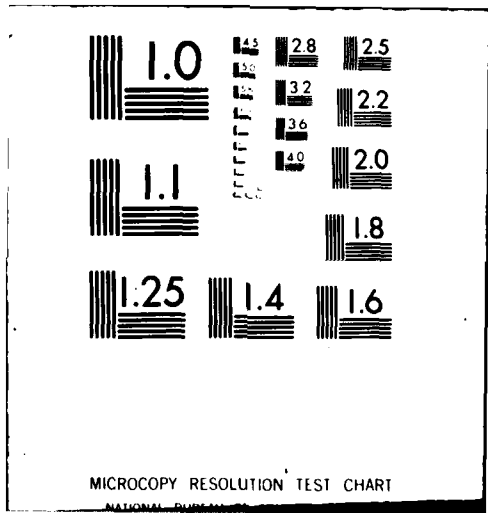
AFGL-TR-81-0337

NL

1-1  
21-00



END  
DATE  
FILMED  
4-82  
DTIC



MICROCOPY RESOLUTION TEST CHART

NATIONAL BUREAU OF STANDARDS-1963-A

12

AFGL-TR-81-0337

AD A 1 1 1 8 0 6

**ANALYSIS OF THE RAM EFFECT OBSERVED WITH THE ELECTRON ESA ON THE S3-2 SATELLITE**

Frederick A. Hanser  
Bach Sellers

Panametrics, Inc.  
221 Crescent Street  
Waltham, Mass. 02254

November 1981  
Final Report  
November 1978 - November 1981

Approved for public release, distribution unlimited.

AIR FORCE GEOPHYSICS LABORATORY  
AIR FORCE SYSTEMS COMMAND  
UNITED STATES AIR FORCE  
HANSCOM AFB, MASSACHUSETTS 01731

DTIC  
ELECTE  
MAR 9 1982  
S B

NO COPY

82 08 09 041

UNCLASSIFIED

SECURITY CLASSIFICATION OF THIS PAGE (When Data Entered)

REPORT DOCUMENTATION PAGE		READ INSTRUCTIONS BEFORE COMPLETING FORM
1. REPORT NUMBER AFGL-TR-81-0337	2. GOVT ACCESSION NO.	3. RECIPIENT'S CATALOG NUMBER
4. TITLE (and Subtitle) Analysis of the Ram Effect Observed with the Electron ESA on the S3-2 Satellite		5. TYPE OF REPORT & PERIOD COVERED Final Report Nov. 1978-Nov. 1981
7. AUTHOR(s) Frederick A. Hanser Bach Sellers		6. PERFORMING ORG. REPORT NUMBER
8. PERFORMING ORGANIZATION NAME AND ADDRESS Panametrics, Inc. 221 Crescent Street Waltham Mass 02254		9. CONTRACT OR GRANT NUMBER(s) Contract F19628-79-C-0009
10. CONTROLLING OFFICE NAME AND ADDRESS Air Force Geophysics Laboratory L.G. Hanscom AFB, Mass. 01731 Contract Monitor: Paul L. Rothwell, PHG		10. PROGRAM ELEMENT, PROJECT, TASK AREA & WORK UNIT NUMBERS 62101F 760109AD
14. MONITORING AGENCY NAME & ADDRESS (if different from Controlling Office)		12. REPORT DATE November 1981
		13. NUMBER OF PAGES 17
		15. SECURITY CLASS. (of this report) UNCLASSIFIED
		15a. DECLASSIFICATION/DOWNGRADING SCHEDULE
16. DISTRIBUTION STATEMENT (of this Report)  Approved for public release, distribution unlimited.		
17. DISTRIBUTION STATEMENT (of the abstract entered in Block 20, if different from Report)		
18. SUPPLEMENTARY NOTES		
19. KEY WORDS (Continue on reverse side if necessary and identify by block number) Electron flux ESA Ram effect S3-2 satellite		
20. ABSTRACT (Continue on reverse side if necessary and identify by block number) <p>&gt; A parallel plate electrostatic analyzer (ESA) to detect 0.08 to 17 MeV electrons was launched on the S3-2 satellite in late 1975. Analysis of the low altitude data revealed that the ESA was responding to the neutral atmosphere through a ram effect. The ram effect was confined to attack angles of less than about 30°, and was generally present only at the lowest altitudes (250-300 km). By excluding</p>		

Unclassified

~~SECURITY CLASSIFICATION OF THIS PAGE (When Data Entered)~~

-- all data with an ESA attack angle of less than  $45^{\circ}$ , completely reliable electron spectra are obtained at all altitudes.

UNCLASSIFIED

~~SECURITY CLASSIFICATION OF THIS PAGE (When Data Entered)~~

## FOREWORD

The work described in this report was originally started as a study to analyze the mechanisms of magnetospheric storm particle energization, using the S3-2 electron ESA data as a primary input. During the course of the initial data analysis the ram effect was discovered and the effort was diverted into studying this phenomenon. A lack of sufficient time resulted in the initial program being delayed and subsequently discontinued. Some data on the ram effect have been analyzed and are presented in this report. The ram effect is understood sufficiently to allow complete analysis of the S3-2 ESA data, providing electron fluxes uncontaminated by ram effect counts. The help of Paul Rothwell, the contract monitor, and of Roger Vancour, in obtaining the S3-2 electron ESA data in various stages of reduction, is appreciated.



Accession For	
DTIC	<input checked="" type="checkbox"/>
AD	<input type="checkbox"/>
AS	<input type="checkbox"/>
NS	<input type="checkbox"/>
Availability Codes	
Dist. 11 and/or	
Dist. Special	
<b>A</b>	

## TABLE OF CONTENTS

	<u>Page</u>
FOREWORD	iii
LIST OF ILLUSTRATIONS	vi
LIST OF TABLES	vi
1. INTRODUCTION	1
2. ANALYSIS OF RAM EFFECT IN THE S3-2 ELECTRON ESA	2
3. DISCUSSION AND CONCLUSIONS	10
REFERENCES	11

<u>Figure No.</u>	LIST OF ILLUSTRATIONS	<u>Page</u>
2.1	Outline of the Detection Assembly of the S3-2 Electron ESA.	3
2.2	Four Count Rate vs Energy Channel Profiles for Less than 16° Attack Angles.	8
2.3	Count Rate vs Attack Angle Profile for Summed Energy Channels 17 to 32 for Part of Orbit 188.	9

<u>Table No.</u>	LIST OF TABLES	<u>Page</u>
2.1	Number Densities for the 800° K Spring/Fall Model Standard Atmosphere	4
2.2	Oxygen Number Densities as a Function of Exospheric Temperature	4
2.3	Atomic and Molecular Energies for a Satellite Velocity of 7.65 km/sec	5
2.4	Incident Flux of Atomic Oxygen and Helium for an 800° K Exospheric Temperature	5
2.5	Some CEM Count Rates for Different Altitudes, Orbital Locations, and Days	6

## 1. INTRODUCTION

An electron ESA to measure 0.08 to 17 keV electrons was launched in late 1975 as part of the payload of the S3-2 satellite. The ESA is of the parallel-plate type with a Channel Electron Multiplier (CEM) detector, and its construction and initial in-orbit operations are described in Refs. 1.1, 1.2, and 1.3. The S3-2 satellite is in a near polar orbit approximately in the noon-midnight meridian, with altitude varying between about 250 km and 1500 km. The S3-2 spin axis is normal to the orbital plane, with the ESA viewing perpendicular to the spin axis. Thus the ESA normally observes almost all pitch angles from  $0^{\circ}$  to  $180^{\circ}$ , and views nearly along the satellite velocity vector once per 20 second spin period.

Initial data from the ESA turn-on and some subsequent auroral zone passes showed completely normal operation. Reduced electron spectra showed the shapes and spatial behavior expected for auroral electrons (Ref. 1.3). Later, data for complete orbits showed some unusual characteristics, generally at lower altitudes. The electron spectra showed a strong peaking in the highest energy channels occurring once per spin period. This was later determined to be occurring when the ESA was viewing in the direction of the satellite velocity vector, and so was ascribed to a ram effect whereby the ESA was detecting ambient neutrals, although at a very low efficiency.

The ram effect is confined to ESA view directions within about  $30^{\circ}$ - $45^{\circ}$  of the satellite velocity vector, so it affects at most about 1/4 of the data. The ram effect does not appear at altitudes above 1000 km, and only rarely in the 500-1000 km altitude range. The analysis of ESA data is thus most reliable when all data within  $30^{\circ}$ - $45^{\circ}$  of the ram direction are excluded. The following section discusses the ram effect in more detail.

## 2. ANALYSIS OF RAM EFFECT IN THE S3-2 ELECTRON ESA

The basic design of the detection assembly for the S3-2 electron ESA is shown in Fig. 2.1. The central area of the deflection plate consists of an open screen to allow passage of most of the high energy electrons through the deflection plate, and so minimize the backscattering and secondary electron production which contribute to background. Since the plate is swept to -10 kV, the secondary electrons produced on the screen can strike the ground plane with 10 keV of energy, and some of these can be backscattered and deflected into the Channeltron detector aperture.

Some typical number densities for O<sub>2</sub>, O, N<sub>2</sub> and He for a Spring/Fall U.S. Standard Atmosphere model, with an 800° K exospheric temperature are given in Table 2.1 (densities are taken from Ref. 2.1). The dominant constituent is O for the 250-500 km region, with N<sub>2</sub> also being important at 250 km. Above 700 km He is dominant. The variation of the O number density with exospheric temperature is shown in Table 2.2. At the higher temperature N<sub>2</sub> becomes increasingly important in the 200-700 km altitude range.

For the S3-2 satellite the orbital velocity is about 7.65 km/sec near perigee. This velocity is much higher than the thermal velocities of the dominant exospheric constituents, and imparts to the ambient species the kinetic energies given in Table 2.3. The particle energies of Table 2.3 are strongly directional, opposite to the satellite velocity vector. The resulting fluxes for O and He, for an 800° K exospheric temperature, are given in Table 2.4. Note that the fluxes at 250-300 km are 4 to 5 orders of magnitude larger than the maximum expected electron fluxes. The data in Table 2.3 show that O, with an incident energy of 4.88 eV, has sufficient energy to produce secondary electrons, which for most metals requires only 2-3 eV. So the large flux of O atoms in Table 2.4 might very well produce some spurious counts in the electron ESA at the lowest satellite altitudes.

Some data on the ram effect in the six highest energy ESA channels (highest deflection plate potentials) are given in Table 2.5. The average counts are for four count sums of  $4 \times 1/64 = 1/16$  second, and for an ESA attack angle (angle of look direction to the velocity vector) of less than 16°. Most of the data in Table 2.5 have negligible contamination by electrons, since the counts from the same pitch angle range, but in the anti-ram direction were much smaller. The exception is for the very lowest count rates at the higher altitudes, which are true electron counts. The data show that the ram effect counts occur primarily at low altitudes, and are variable. On occasion a suggestion of a ram effect shows up as high as 750 km, as shown by the orbit 528 data.

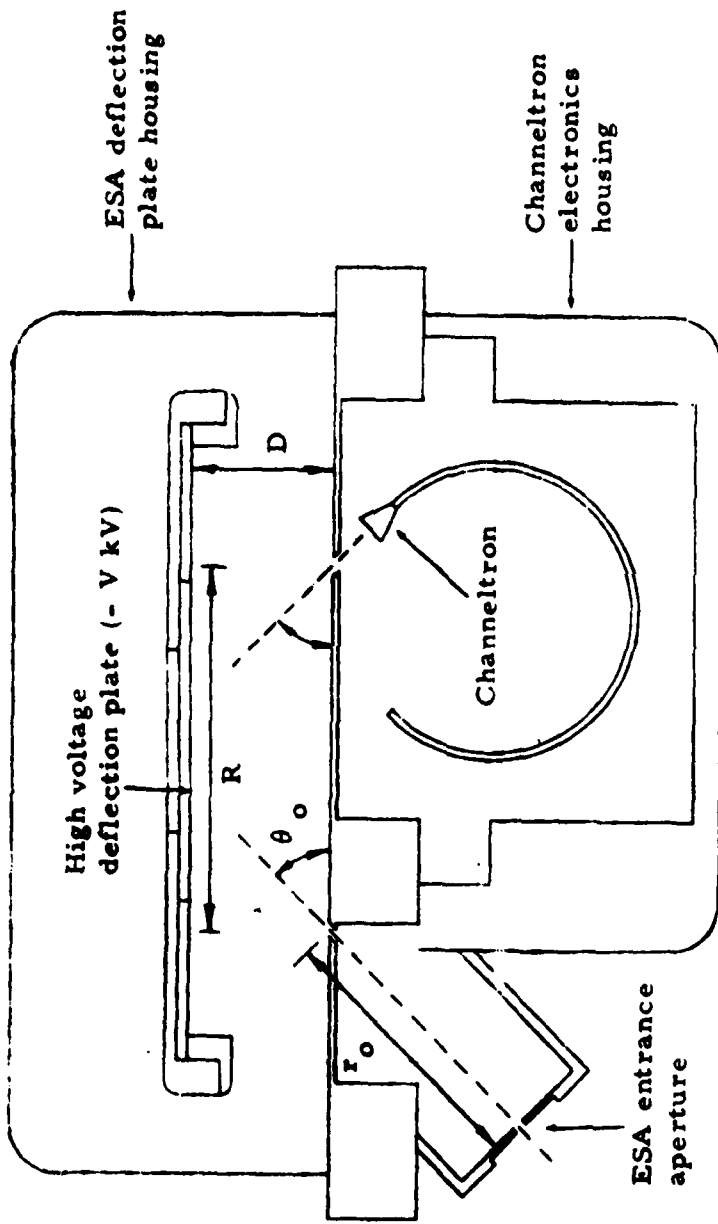


Figure 2.1. Outline of the Detection Assembly of the S3-2 Electron ESA.

Table 2.1

Number Densities for the 800° K  
Spring/Fall Model Standard Atmosphere

Altitude (km)	Number density (#/m <sup>3</sup> ) for*			
	O <sub>2</sub>	O	N <sub>2</sub>	He
200	3.00 × 10 <sup>14</sup>	3.29 × 10 <sup>15</sup>	2.90 × 10 <sup>15</sup>	1.17 × 10 <sup>13</sup>
250	2.98 × 10 <sup>13</sup>	1.02 × 10 <sup>15</sup>	3.82 × 10 <sup>14</sup>	8.59 × 10 <sup>12</sup>
300	3.33 × 10 <sup>12</sup>	3.38 × 10 <sup>14</sup>	5.60 × 10 <sup>13</sup>	6.50 × 10 <sup>12</sup>
500	7.80 × 10 <sup>8</sup>	5.16 × 10 <sup>12</sup>	3.71 × 10 <sup>10</sup>	2.28 × 10 <sup>12</sup>
700	2.94 × 10 <sup>5</sup>	1.00 × 10 <sup>11</sup>	3.74 × 10 <sup>7</sup>	8.51 × 10 <sup>11</sup>
1000	4.84 × 10 <sup>0</sup>	4.06 × 10 <sup>8</sup>	2.43 × 10 <sup>3</sup>	2.15 × 10 <sup>11</sup>

\*Taken from Ref. 2.1.

Table 2.2

Oxygen Number Densities as a Function  
of Exospheric Temperature

Altitude (km)	O Number density (#/m <sup>3</sup> ) for exospheric temperature of*					
	600° K	800° K	1000° K	1300° K	1700° K	2100° K
200	2.56 × 10 <sup>15</sup>	3.29 × 10 <sup>15</sup>	3.70 × 10 <sup>15</sup>	3.86 × 10 <sup>15</sup>	3.73 × 10 <sup>15</sup>	3.59 × 10 <sup>15</sup>
250	5.52 × 10 <sup>14</sup>	1.02 × 10 <sup>15</sup>	1.41 × 10 <sup>15</sup>	1.73 × 10 <sup>15</sup>	1.80 × 10 <sup>15</sup>	1.77 × 10 <sup>15</sup>
300	1.28 × 10 <sup>14</sup>	3.38 × 10 <sup>14</sup>	5.79 × 10 <sup>14</sup>	8.57 × 10 <sup>14</sup>	9.98 × 10 <sup>14</sup>	1.03 × 10 <sup>15</sup>
500	4.86 × 10 <sup>11</sup>	5.16 × 10 <sup>12</sup>	2.04 × 10 <sup>13</sup>	6.46 × 10 <sup>13</sup>	1.32 × 10 <sup>14</sup>	1.86 × 10 <sup>14</sup>
700	2.54 × 10 <sup>9</sup>	1.00 × 10 <sup>11</sup>	8.71 × 10 <sup>12</sup>	5.71 × 10 <sup>12</sup>	2.07 × 10 <sup>13</sup>	4.11 × 10 <sup>13</sup>
1000	1.64 × 10 <sup>6</sup>	4.06 × 10 <sup>8</sup>	1.06 × 10 <sup>10</sup>	1.93 × 10 <sup>11</sup>	1.55 × 10 <sup>12</sup>	5.05 × 10 <sup>12</sup>

\*Taken from Ref. 2.1.

Table 2.3

Atomic and Molecular Energies for a Satellite  
Velocity of 7.65 km/sec

<u>Particle Specie</u>	<u>Particle Mass (amu)</u>	<u>Particle Kinetic Energy (eV)</u>
H	1.008	0.31
He	4.003	1.22
N	14.007	4.27
O	15.999	4.88
N <sub>2</sub>	28.013	8.54
O <sub>2</sub>	31.999	9.76

Table 2.4

Incident Flux of Atomic Oxygen and Helium  
for an 800° K Exospheric Temperature

<u>Altitude (km)</u>	<u>Particle fluxes, #/(cm<sup>2</sup>-sec), for a satellite velocity of 7.65 km/sec</u>	
	<u>j(O)</u>	<u>j(He)</u>
200	$2.52 \times 10^{15}$	$8.95 \times 10^{12}$
250	$7.80 \times 10^{14}$	$6.57 \times 10^{12}$
300	$2.59 \times 10^{14}$	$4.97 \times 10^{12}$
500	$3.95 \times 10^{12}$	$1.74 \times 10^{12}$
700	$7.65 \times 10^{10}$	$6.51 \times 10^{11}$
1000	$3.11 \times 10^8$	$1.64 \times 10^{11}$

Table 2.5

Some CEM Count Rates for Different Altitudes,  
Orbital Locations, and Days

<u>UT</u> <u>(hrs: min)</u>	<u>Altitude</u> <u>(km)</u>	<u>L</u> <u>range</u>	<u>Average counts/(4 readouts),</u> <u>for &lt; 16° attack angle</u>		
			<u>Ch 31-32</u>	<u>Ch 29-30</u>	<u>Ch 27-28</u>
Orbit 188, 12/19/75					
0455	1445 ± 22	8.4-14.5	0.07	0.14	0.29
0505	1565	18-21	0.00	0.00	1.00
0548	355 ± 28	5.0-9.5	103.5	61.6	47.6
0551	309 ± 13	10.3-14.5	124.9	69.0	57.1
0553	280 ± 8	15-16	80.5	50.0	38.7
0555	266 ± 4	8.9-14.3	78.5	46.3	35.2
0557	263 ± 2	5.5-8.7	75.4	39.3	28.2
0559	272 ± 4	3.9-4.8	81.9	47.8	38.4
0601	291 ± 10	2.6-3.4	100.2	66.2	54.1
Orbit 528, 1/12/76					
1054	758 ± 46	8.7-9.0	7.13	4.38	3.13
1144	1198 ± 22	6.8-9.3	0.13	0.00	0.25
1151	939 ± 27	13-18	0.90	1.10	0.90
Orbit 1144, 2/25/76					
0817	243 ± 2	4.5-7.1	3.45	3.10	2.33
0818	247.5 ± 2.5	7.1-8.9	31.0	12.3	11.0
0819	255 ± 5	8.9-13	38.3	18.6	13.3

The period of late 1975 - early 1976 is near solar sunspot minimum, and using the detailed procedure of Ref. 2.1 the base exospheric temperature for the data in Table 2.5 is near 800 K. There is a substantial diurnal variation in the exospheric temperature, with the daytime maximum being near 1000°K. Some of the variations in Table 2.5 are thus due to the substantial latitude/longitude variations in the exospheric temperature.

A more detailed view of the ram effect as a function of energy channel is given in Fig. 2.2, where four sets of low altitude (250-300 km) data are plotted. Since the energy channel number is proportional to the logarithm of the detected electron energy (and the deflection plate voltage - a range of 2.3 decades), the response to the ram effect is approximately proportional to the deflection plate voltage. The angular response of the ram effect for energy channels 17 to 32 is plotted in Fig. 2.3. The plot is split into two parts and shows that for this location in the orbit the ram count maximum is for an attack angle of 7° after the minimum attack angle. It has not been determined which direction this angle of incidence corresponds to in Fig. 2.1 (+ or - to  $\theta_0$ ), since this requires having detailed information on the orientation of the ESA on the S3-2 satellite, as well as information on the direction of the satellite's spin vector. This information was not readily available.

The actual angular response of the ESA to electrons has a full width of only about 6°, so the data in Fig. 2.3 suggest that the ram effect counts are produced primarily by neutral atoms which have undergone some scattering before they strike the deflection plate. There appears to be no ram effect for angles more than 25° before the minimum attack angle, but some ram effect is noticeable to about 35° after the minimum attack angle. By excluding from analysis all data with an attack angle of < 45°, there should be no contamination in the resulting electron spectra. For altitudes above 1000 km this data exclusion is not necessary and all data can be analyzed.

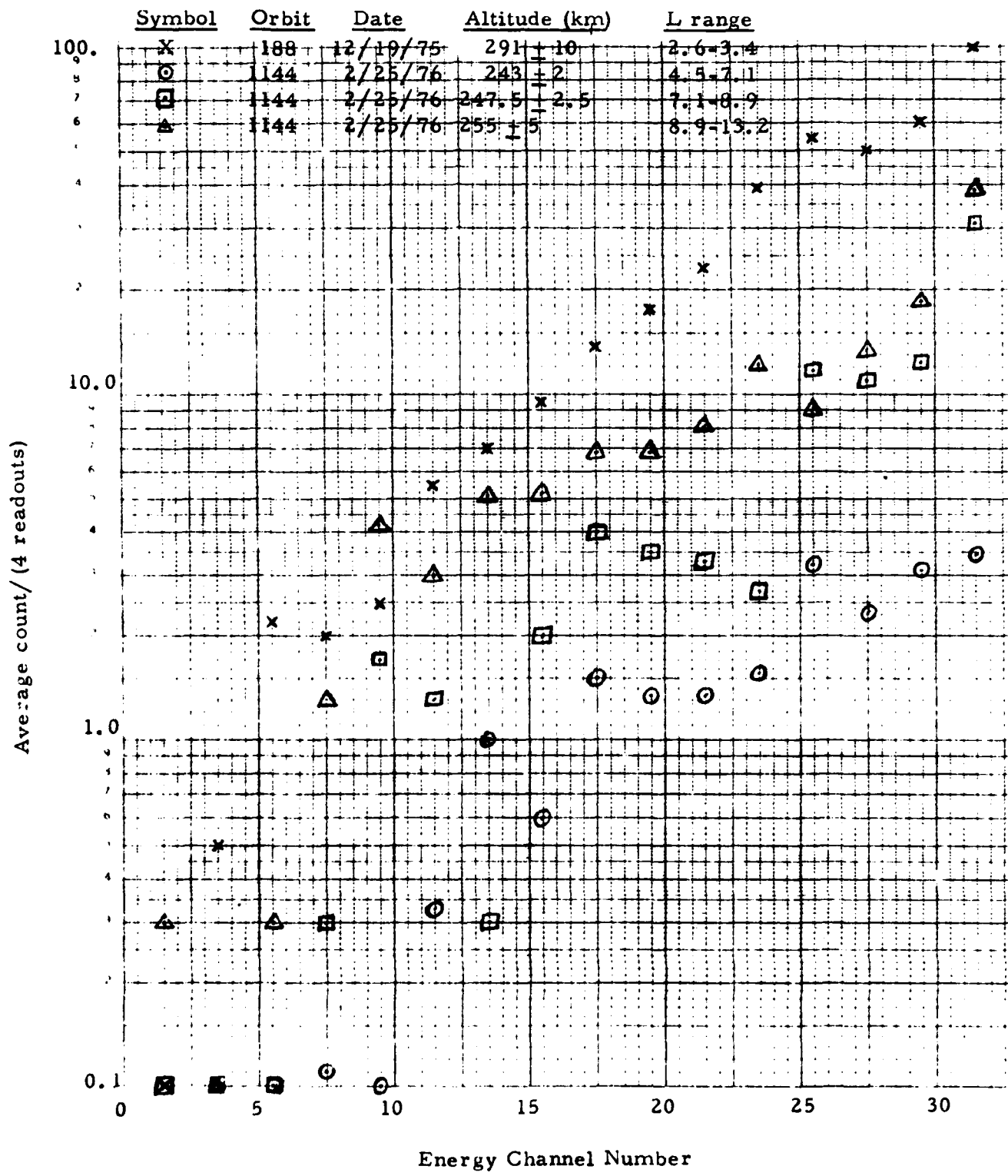


Figure 2.2. Four Count Rate vs Energy Channel Profiles for Less than 16° Attack Angles.

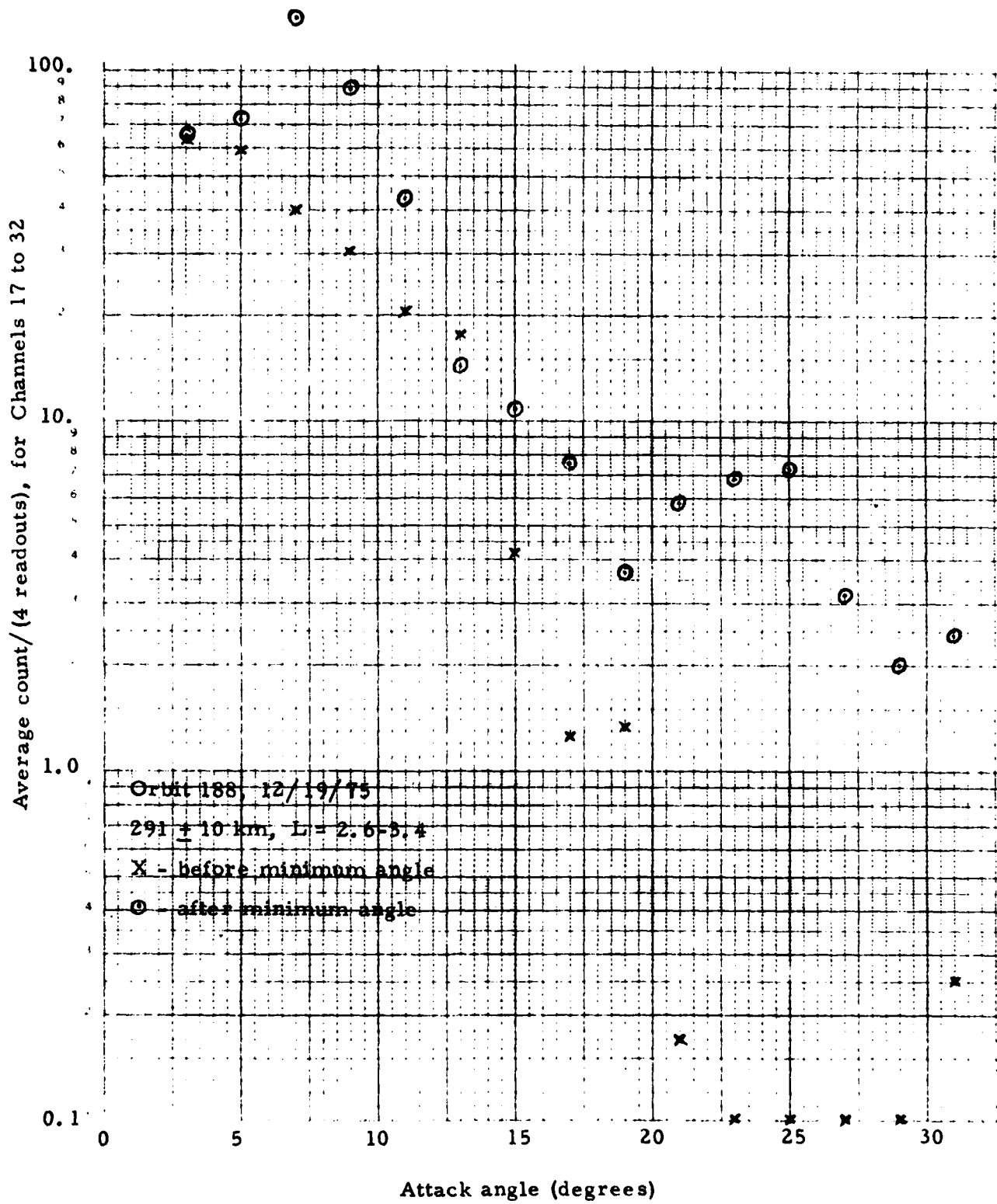


Figure 2.3. Count Rate vs Attack Angle Profile for Summed Energy Channels 17 to 32 for Part of Orbit 188.

### 3. DISCUSSION AND CONCLUSIONS

The ram effect observed in the S3-2 ESA is primarily due to the large velocity required for satellites in the few hundred km altitude region. The satellite velocity gives the dominant neutral oxygen atoms an energy of about 5 eV when they are swept up, and this is sufficient to produce secondary electrons which can then be detected. The ram effect has also been observed on other satellites, in particular the Low Energy Electron Experiment on the Atmospheric Explorer -C (AE-C) satellite (Refs. 3.1 and 3.2). The AE-C experiment used cylindrical electrostatic analyzers, and they produced ram effect counts for attack angles of less than  $20^\circ$ . Data analysis was only performed for attack angles greater than  $45^\circ$  (Ref. 3.2). The AE-C experiment also proved sensitive to sunlight ( $< 20^\circ$ ), and to scattered UV (mostly H Lyman alpha) from the earth's atmospheric horizons. The S3-2 ESA shows no sensitivity to either direct sunlight or to scattered UV.

The electron ESA on the S3-2 satellite shows a ram effect in the 250-300 km altitude range for attack angles up to  $25-35^\circ$ . The ram effect is occasionally observed at altitudes up to 750 km. Exclusion of all data for attack angles  $< 45^\circ$  for altitudes  $< 1000$  km should eliminate any contribution of the ram effect to the reduced electron spectra. This mode of data analysis would allow the use of the ESA data for auroral electron flux studies.

The ram effect itself could be used for a detailed study of the neutral atmospheric density in the 250-500 km region. The S3-2 satellite provided about two years of reliable data, so the ram effect data should provide density information for that time period for the noon-midnight polar meridian. The data could be used to relate density to the exospheric temperature distribution, and observe the effects of solar and geomagnetic activity.

## REFERENCES

- 1.1 P. R. Morel, F. A. Hanser, and B. Sellers, "Design, Fabrication, and Integration of an Electrostatic Analyzer for a Satellite Payload," Scientific Report No. 1, AFCRL-TR-75-0017 (Dec. 1974). AD A 006698.
- 1.2 P. R. Morel, F. A. Hanser, and B. Sellers, "An Electrostatic Analyzer for an Air Force Satellite Payload," Scientific Report No. 2, AFCRL-TR-75-0366 (July 1975). AD A 015798
- 1.3 F. A. Hanser, and B. Sellers, "An Electrostatic Analyzer for an Air Force Satellite Payload - Evaluation of In-Flight Operation," Final Report, AFGL-TR-76-0203 (July 1976). AD A 013313
- 2.1 U. S. Standard Atmosphere Supplements, 1966, U. S. Government Printing Office, Washington, D. C.
- 3.1 R. A. Hoffman, J. L. Burch, and R. W. Janetzke, "AE-LEE measurements at low and midlatitude," in Proceedings of the Workshop on Electron Contamination in X-Ray Astronomy Experiments, S. S. Holt, ed., GSFC Report X-661-74-130 (May, 1974).
- 3.2 D. G. Torr, M. R. Torr, R. A. Hoffman, and J. C. G. Walker, "Global Characteristics of 0.2 to 26 keV Charged Particles at F Region Altitudes," Geophys. Res. Lett. 3, 305-8 (1976).